

Homogenous Dual-Ligand Zinc Complex Catalysts for Chemical Fixation of CO₂ to Propylene Carbonate

Yan-Li Shi¹ · Peng Zhang¹ · Ding-Hua Liu¹ · Peng-Fei Zhou¹ · Lin-Bing Sun¹

Received: 4 May 2015 / Accepted: 18 June 2015
© Springer Science+Business Media New York 2015

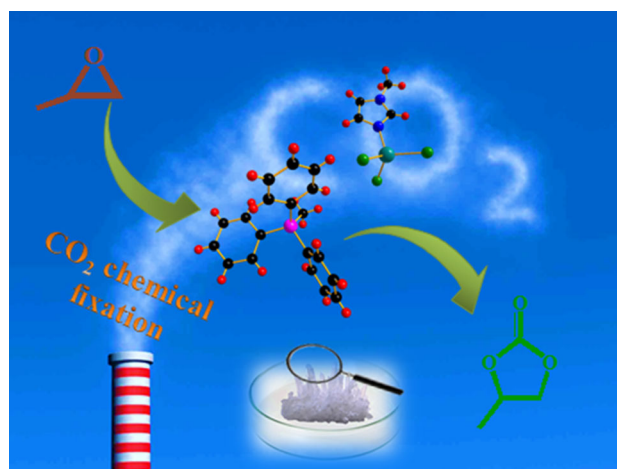
Abstract Homogeneous dual-ligand zinc complex catalysts were developed for the synthesis of propylene carbonate (PC) through chemical fixation of CO₂. It was found that among a number of various pK_a N-donor ligands, the catalytic performance was enhanced dramatically and the corrosion of the reaction system was effectively inhibited when 1-methylimidazol (IMI) was used as the N-donor ligand, in which >90 % PC yield could be obtained under mild reaction conditions. The dual-ligand zinc complex catalysts were characterized by various spectroscopic techniques such as FT-IR and ¹HNMR. X-ray crystallography showed that the Zn(II) atom was coordinated in tetrahedron geometry by three bromine atom, one IMI nitrogen atom, and one crystallographically independent cation to give a 3D tetrahedron structure, which forms tetracoordinated complexes. The structure of the complex gives the reasons for the enhancement of the catalytic activity from the microscopic molecular structure point of an extremely long and therefore labile Zn–Br bond, the diversification of the bond angles, and the interplay between the steric hindrance, which have great influence on the interaction forces of Zn–Br.

Electronic supplementary material The online version of this article (doi:10.1007/s10562-015-1565-9) contains supplementary material, which is available to authorized users.

- ✉ Ding-Hua Liu
ncldh@njtech.edu.cn
- ✉ Lin-Bing Sun
lbsun@njtech.edu.cn

¹ State Key laboratory of Materials-Oriented Chemical Engineering, College of Chemistry and Chemical Engineering, Nanjing Tech University, Nanjing 210009, China

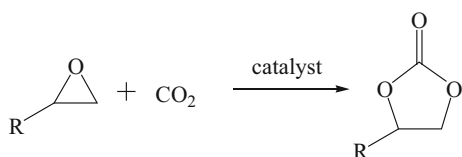
Graphical Abstract



Keywords Dual-ligand zinc complex · Carbon dioxide · Propylene carbonate

1 Introduction

Carbon dioxide is naturally abundant, nontoxic, non-flammable, cheap and easily accessible, making it an attractive “regenerative” C1 feedstock that can replace oil-based raw materials [1, 2]. Therefore, the chemical fixation of CO₂ is of great significance from the viewpoint of better utilization of C1 sources and environment concern. One of the few commercial routes [3, 4] using CO₂ as a raw material in this area is the insertion of CO₂ into epoxides to afford five-membered cyclic carbonates (Scheme 1) which have been widely used as electrolytes in secondary batteries,



Scheme 1 Synthesis of cyclic carbonate using CO_2 and epoxide

intermediates in organic synthesis, monomers for synthesizing polycarbonate, polar aprotic solvents, alkylating agents and building blocks for biologically active pharmaceutical agents [5–10].

For this reaction, various catalytic systems have been developed that include homogeneous and heterogeneous catalytic systems. The homogeneous catalysts [11–24] include salen, porphyrin, phthalocyanine and other complexes of the main group and transition metals (Zn, Al, Cr, Co, Cu, Ni and Sn), as well as quaternary ammonium salts, ionic liquids and polyoxometalates. However, these usually suffer from drawbacks such as low catalytic activity/selectivity, high temperature and pressure, water sensitivity and importantly for industrial application the corrosion of the catalyst to the reactor materials is so serious. For many years, in order to overcome these drawbacks various catalytic systems have been studied. Many kinds of base additives for use as promotional co-catalysts (such as amines and pyridines) have been investigated, as well as immobilized metal salt catalysts on inorganic or organic solid materials [17, 18, 25–33]. Mo et al. studied the effect of different N-donor ligands in oxidative carboxylation of methanol and the catalysts show relatively high catalytic activities and inhibition of corrosion [34]. According to the investigations of Kim et al. and Sun et al., P-donor ligands also exhibited highly promotion effect for chemical fixation of CO_2 to cyclic carbonate [35, 36]. These reports mainly focus on single-ligand complexes, even though some co-catalysts were added to improve the catalytic activity. However, less attention is given to the structure of dual-ligand complexes. This is the first report about the dual-ligand complex and its crystalline structure; moreover, the dual-ligand complex exhibits high catalytic activity and inhibition of corrosion for the synthesis of PC.

In this paper, we report a strategy to modulate the properties of a new dual-ligand zinc complex by introducing electron withdrawing groups. Phosphine ligand and various $\text{p}K_{\text{a}}$ values to N-donor ligands [37] were introduced

to the $\text{CH}_3\text{CH}_2\text{OH}$ solution containing ZnBr_2 and participated in the crystallization of the dual-ligand zinc complex (Scheme 2). A new kind of zinc complex was thus fabricated in which phosphine ligand acts as active ligand and N-donor ligand plays an important role in both catalytic activity and corrosion inhibiting ability. Our results also demonstrate that the dual-ligand zinc complex is highly active for the cycloaddition of CO_2 to epoxides. More importantly, the corrosion speed is dropt heavily. Moreover, they were successfully characterized by using various analytical techniques. X-ray crystallographic studies reveal that the complex units connected by one N-donor (IMI^+) ligand, one methyltriphenylphosphonium (MTP^+) cation and three Br^- ions to give a 3D tetrahedron structure with a Zn/P/N ratio of 1:1:1, which results in an obvious improvement of activity from the molecular structure point.

2 Experimental

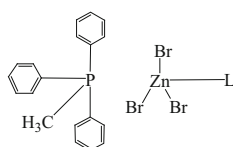
2.1 Materials and Equipment

Carbon dioxide was supplied by Ruier Special Gas Ltd. with a purity of 99.99 %. All other chemicals were obtained commercially without further purification. The FT-IR spectra of compounds were recorded with a Nicolet Impact 410 FT-IR spectrometer with pressed KBr pellets in the $4000\text{--}500\text{ cm}^{-1}$ regions. The single crystals of compounds were singled out by visual examination under the microscope and glued at the top of a thin glass fiber with epoxy glue in air for data collection, and the collection of crystallographic data was carried out on a Bruker Apex 2 CCD with Mo $K\alpha$ radiation ($\lambda = 0.071073\text{ nm}$) at 296 (2) K via ω - 2θ scan method. The crystal structures were solved by direct method and refined on F2 by full-matrix least-squares methods using the SHELX97 program package. The $^1\text{H NMR}$ spectra was recorded on a Bruker Avance III 400 M spectrometer, using CDCl_3 as the solvent with a TMS internal standard or residual solvent peak as the reference.

2.2 Sample Preparation

The sample was prepared by mixing an acidic field alcoholic solution of methyltriphenylphosphonium bromide (MTPB), L and ZnBr_2 in the ratio of 1:1:1, named **1e** (L = IMI), while the molar ratio between ZnBr_2 and ligand is 1:2 for the single-ligand complex catalysts. The solution was kept at 343 K for 1 h. Small transparent crystals were obtained upon gradual cooling to room temperature. The product was washed with a mixture of diethyl ether and ethanol, redissolved in ethanol and kept at

Scheme 2 Structure of the catalysts (L denotes N-donor ligand)



305 K for 1 week to crystallize. The obtained crystals were washed, dried and kept under vacuum.

Complex **1e**: ¹HNMR (CDCl₃, 400 Hz), δ_Hppm 3.267–3.300 (d, 3H, N–CH₃), 6.911 (s, H, ring N–CH–N), 7.363–7.588 (m, 2H, ring C–CH–N), 3.725 (s, 3H, P–CH₃), 7.735 (m, 15H, ring ArH).

2.3 General Procedure for the Synthesis of PC

In a typical reaction, the cycloaddition reaction of CO₂ to PO was carried out in a stainless steel autoclave (1 L inner volume). PC was added before the reaction in order to form a circular reaction system, which simulated the actual production process. Prior to the reaction, the catalyst was evacuated at 373 K for 1 h, CO₂ (liquid, 2.5 MPa) was introduced to a mixture of PO and PC with a molar ratio of 1:3. The gauge was used to monitor the pressure of the system. The initial pressure was generally adjusted to 4 MPa at 373 K, and the autoclave was heated at that temperature for 1 h. After cooling, the excess gases were vented, and the liquid products were analyzed by gas chromatography (GC). GC analysis was performed using Agilent GC 7890A equipped with a flame ionization detector (FID) and a HP-5 column (length = 30 m, inner diameter = 0.32 mm, film thickness = 0.25 μm), and the side-products were detected by 5973 GC–MS with chemstation containing a NIST Mass Spectral Database. Each catalytic reaction was repeated three times to secure reproducibility.

2.4 Corrosion Inhibition

During the reaction, the rate of corrosion, in g/(m² h), was measured by a standard method described in ASTM No. B575. Test pieces (about 20 mm × 10 mm × 3 mm) of 10 (C 0.08 %, Mn 0.37 %, Si 0.20 %, S 0.03 %, P 0.035 %, Cr 0.13 %, Ni 0.23 %, Cu 0.25 % from Baosteel, China); 316 (C 0.08 %, Cr 17.0 %, Mn 1.6 %, Si 1.0 %, P 0.035 %, Ni 11.5 %, S 0.03 %, from Baosteel, China) were introduced into the autoclave using a special sample cage. Corrosion data were obtained at 418 K after 72 h of reaction with the acidic environment of constantly introducing CO₂ gas. Each corrosion reaction was repeated three times to secure reproducibility and the experimental error about the weight-loss of the sample is less than 5 %. The corrosion speed was calculated using the following equation:

$$V = (m_0 - m)/St = \Delta m/St$$

V is the corrosion speed, g/(m² h); m₀ is the sample's quality before reaction, g; m is the sample's quality after reaction, g; S is the sample's area, m²; t is the reaction time, h.

3 Results

3.1 Effects of Various N-Donor Ligands

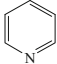
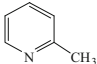
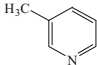
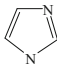
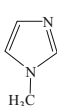
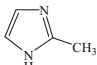
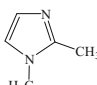
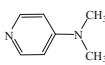
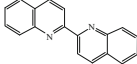
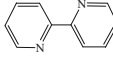
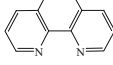
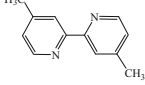
Effects of various N-donor ligands in catalytic performance of basic ZnBr₂ and MTPB for synthesis of PC have been investigated by testing the catalytic activity (Table 1; Fig. 1). In order to determine the acidity of the solution, the pH values before and after the reaction were detected. The corrosion rate of a relatively alkaline environment will be more slowly.

Figure 1 shows that among monodentate ligands, the yield of PC increases with the more strong basicity (pK_a) and then decreases. **1e** exhibits the highest catalytic activity, corresponding to a yield of 92.1 %. This data is the highest one among all of the N-donor ligand systems investigated. However, **1d** shows the lowest activity, corresponding to a lowest yield of 72.3 %. Among the polydentate ligand systems, the relationship between the yield of PC and pK_a is also the same. **2c** catalyst shows the highest activity, with a yield of 87.8 %. Compared with **3** and **4** catalysts, which contain only one additive, the catalytic activity is enhanced with the addition of various N-donor ligands, especially in the case of IMI. It is worth noting that most of the catalysts presented excellent selectivity (>98 %) towards PC. The results of GC–MS suggest that there is only tiny amount of propylene glycol acting as the by-product. On the basis of these results, it is clear that the catalytic activity is enhanced in various degrees, and both of the two ligands play synergistic effects in the enhancement of catalytic performance.

3.2 Characterization and Structural Studies of Dual-Ligand Zinc Complex

Characterization details of complex **1e** are explained here. The Fourier transform infrared spectroscopic (FT-IR) of the MTPB, **3**, **1e**, and **4** are presented in Fig. 2. All of the samples were dried under vacuum at 60 °C for 24 h before being detected. All the FT-IR spectra show characteristic vibration bands at around 1650 and 400 cm⁻¹. MTPB displays a characteristic band of P–Br centered at 566 cm⁻¹ peak, while the other catalysts do not, which demonstrates a complete reaction with ZnBr₂. In addition, the band at 3120 cm⁻¹ can be attributed to the stretching vibration of N–H in **4**. It is worth noting that the characteristic band of N–H becomes invisible, instead of some slightly Ph–H bands at around 3160 and 2900 cm⁻¹ in **1e**. Besides, strong band at 622 cm⁻¹ is observed for **1e**, which can be assigned to Zn–N vibrations. The stretching vibration of the C=N double bonds appear at 1619 cm⁻¹ for IMI [38]. The stretching vibrations of the C=N double bonds

Table 1 Effects of N-donor ligands on the catalytic activities

Catalyst	Category	Ligand	Structure ^a	pK _a ^a	pH ^b	pH ^c	Yield ^d (%)	Selectivity ^d (%)
1a	Monodentate	Pyridine (Py)		5.17	5.79	7.02	74.5	97
1b		2-Methylpyridine (2MP)		5.539	5.86	7.19	79.6	98
1c		3-Methylpyridine (3MP)		5.68	5.93	7.29	82.7	98
1d		Imidazole (IM)		6.95	6.07	8.16	72.3	98
1e		1-Methylimidazol (1MI)		7.06	6.11	8.24	92.1	99
1f		2-Methylimidazole (2MI)		7.86	6.49	8.17	82.3	98
1g		1,2-Dimethylimidazole (DMI)		8.20	6.75	8.31	79.6	98
1h		4-Dimethylaminopyridine (DMAP)		9.70	6.97	8.55	76.4	99
2a	Polydentate	2,2'-Biquinoline (BQI)		3.3	5.62	6.14	62.7	94
2b		2,2-Bipyridine (BPy)		4.35	5.71	6.61	71.4	95
2c		1,10-Phenanthroline monohydrate (Phen)		4.86	5.76	7.07	87.8	99
2d		4,4'-Dimethyl-2,2'-dipyridyl (MBPy)		5.1	5.84	7.15	67.3	96
3^e		No		–	5.89	6.57	71.8	98
4^f		1-Methylimidazol (1MI)		7.06	6.33	7.95	74.2	98

Reaction conditions: catalyst (0.04 mol%), PO (0.5 mol), PC (3 mol), temperature (373 K), CO₂ pressure (4.0 MPa), reaction time (1 h)

^a Structure and pK_a value of the ligand

^b pH value of the reaction system before the reaction

^c pH value after the reaction

^d Determined by GC

^e Catalyst (0.04 mol%); n(ZnBr₂):n(MTPB) = 1:2

^f Catalyst without MTPB

appear at 1635 cm⁻¹ for **4**, respectively. Wang et al. [39] reported that a blue shift for the stretching vibrations of the C=N double bonds were caused by ferric ions. Therefore, FT-IR data provide evidence for the existence of strong ligand interactions between the P-donor and N-donor ligands and zinc ions.

Further information of **1e** is provided by X-ray diffraction. The crystal structure data are summarized in Table 2.

The atomic coordinates and equivalent isotropic thermal parameters are listed in Table S1, while the bond distances and bond angles are presented in Table S2. Single-crystal X-ray indicates that the complex with a formula. As shown in Fig. 3, the asymmetric structure unit in the tetrahedron contains one Zn²⁺ ion, three Br⁻ ions, one 1MI⁺ N-donor ligand and one crystallographically independent (MTP)⁺ cation, which forms four-coordination complexes. The

Fig. 1 Relationship between pK_a of **a** monodentate and **b** polydentate ligands and the yield of PC

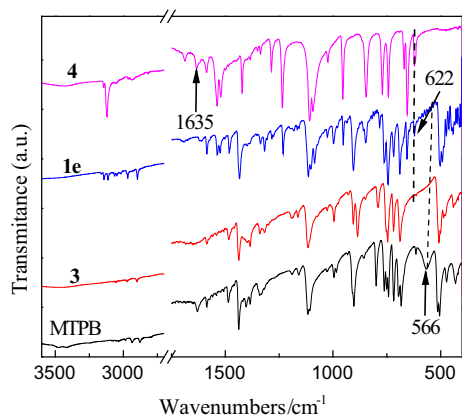
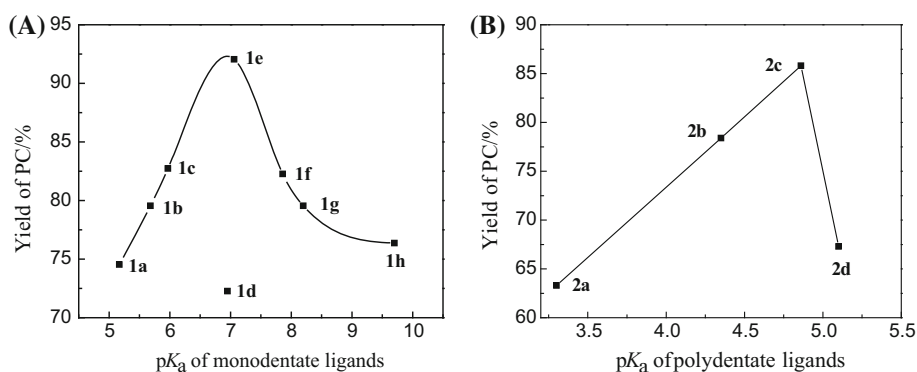


Fig. 2 FT-IR spectra of ligands and catalysts

independent (MTP)⁺ cation composed of three planar phenyl groups and one methyl group around the central phosphorus atom in the form of a distorted tetrahedron. The interplay between the steric hindrance, a repulsive effect resulting from the large size of the phenyl groups, and the Van-der-Waals forces stabilize the structure. The anions arranged to form a cavity. Figure 3 demonstrates the arrangement of the anions and cations. The anion is significantly disordered, as shown by the large bromine atom ellipsoids. The smaller central atom of the anion implies that the disorder, if dynamic, is primarily librational, involving in a distorted tetrahedral configuration by three Br⁻ ligands and the IMI⁺ N-donor ligand. The bond lengths and bond angles of the cation are slightly different, as seen in Table S2. The tetrahedral anion has bond lengths in the range between 1.8004 and 1.8224 Å and the bond angles range between 108.484 and 109.943°, which reveals their distortion. This distortion may be attributed to the steric hindrance induced by the surrounding cations. The bond lengths of Br–Zn (Br1–Zn1 = 2.4492(21), Br3–Zn1 = 2.4127(24)) are longer than that in zinc bromide. The bond angles of Br–Zn–Br (Br2–Zn1–Br3 = 114.978(61), Br1–Zn1–Br2 = 109.046(37)) are larger than that in [(CH₃)(C₆H₅)P]ZnBr₄ which shorten the angles

Table 2 X-ray data collection parameters and refinement of **1e**

Chemical formula (moiety)	C ₁₉ H ₁₈ P, C ₄ H ₆ Br ₃ N ₂ Zn
Chemical formula (sum)	C ₂₃ H ₂₄ Br ₃ N ₂ PZn
Formula mass	664.510/g/mol
Crystal system	Monoclinic
a (Å)	9.406 (9)
b (Å)	27.12 (3)
c (Å)	10.372 (10)
Alpha (°)	90.000
Beta (°)	91.806 (13)
Gamma (°)	90.000
Unit cell volume (Å ³)	2644.49 (400)
Temperature (K)	296 (2)
Space group	P121/n1 (14)
No. of formula unit in unit cell (Z)	4
No. of reflections measured	16756
No. of independent reflections	4580
R _{int}	0.1210
Final R1 values (I > 2σ(I))	0.0553
Final wR2 values (I > 2σ(I))	0.1280
Final R1 values (all data)	0.1226
Final wR2 values (all data)	0.1678

between Br–Zn–N with no doubt [40]. On the basis of the discussion above, the interplay between the steric hindrance, the exceptionally long Zn–Br bond, and the diversification of the bond angles may have great influence on the interaction forces of Zn–Br. According to the mechanism, these factors are considered to be responsible for the enhanced catalytic performance.

3.3 Effect of Reaction Conditions

The reaction conditions such as the influence of molar ratio, temperature, CO₂ pressure and reaction time on the chemical fixation of CO₂ to PC were investigated to find the most appropriate and efficient reaction conditions.

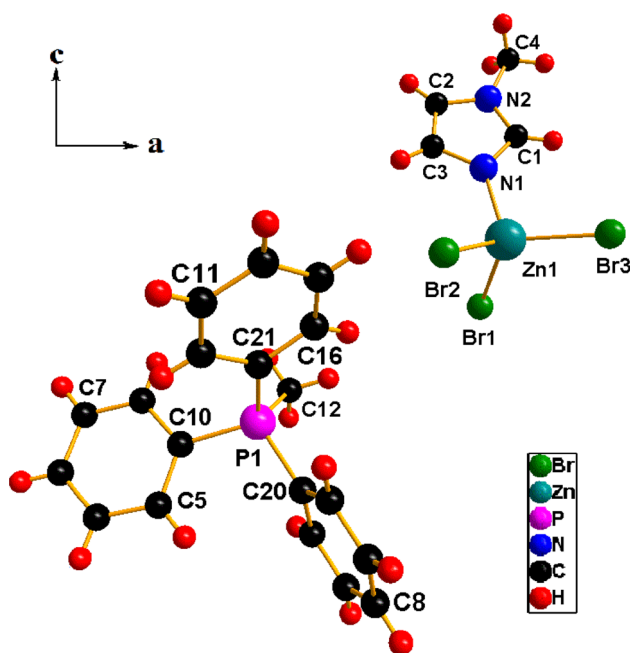


Fig. 3 Structure view of **1e**

Figure 4 shows the effect of the molar ratio between ZnBr_2 and 1MI. All of the experiments were carried out on equal terms of MTPB and the molar ratio between ZnBr_2 and MTPB is 1:1. The results indicate that the molar ratio of the catalyst has a significant impact on the reaction. The yield of PC reaches its highest with >98 % selectivity when the ratio of ZnBr_2 :1MI reaches 1:1. Further increase in the concentration of 1MI causes a decrease in the yield, which may be due to excess 1MI saturating the catalyst binding positions, thus leaving no room for the binding of epoxide to the catalyst for further activity.

Figure 5 shows the effect of temperature on the catalytic activity and it is sensitive to reaction temperature, in which

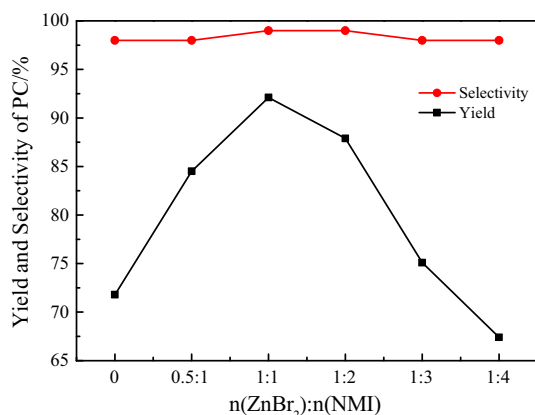


Fig. 4 Effect of molar ratio. Reaction conditions: catalyst (0.04 mol%), PO (0.5 mol), PC (3 mol), temperature (373 K), CO_2 pressure (4.0 MPa), reaction time (1 h)

the PC yield increases sharply with increasing temperature from 333 to 373 K. However, further increase in temperature causes a decrease of the yield and the selectivity. It is plausible that the decrease of PC yield is a result of side reactions under higher temperature, such as PC polymerization, PO isomerization, and a reaction between PO and water [41]. GC-MS confirmed that a tiny amount of propylene glycol acting as the by-product. Therefore, from a practical standpoint the optimal reaction temperature is 373 K.

The effect of CO_2 pressure was also investigated under the same reaction conditions (Fig. 6). As seen, pressure has a great influence on the yield of PC upon varying the CO_2 pressure in the range 2.5–4.0 MPa, whereas the yield changes only slightly with >98 % selectivity in the range 4.0–5.0 MPa. A similar influence of CO_2 pressure on catalytic activity has been observed in other catalytic systems in the literature [41, 42]. Based on the reports, PO and PC should be in their liquid form under the reaction conditions adopted. Lower CO_2 pressure could reduce the absorption of CO_2 in the solution of the catalyst. Higher CO_2 pressure enhanced PC yield due to the higher CO_2 concentration in the liquid phase of the reaction system. The considerable drawbacks of using CO_2 as a reagent in organic synthesis are the potential dangers associated with high-pressure operations. The experimental results above demonstrate that the reaction can be operated smoothly at relatively low pressure in the presence of catalyst **1e**.

The dependence of PC yield on reaction time was also investigated under identical reaction conditions. As shown in Fig. 7, the yield of PC increases rapidly in the initial stage and stays almost steady after 1 h. Meanwhile, nearly all the PO could be converted within 1 h. Conclusively, a reaction time of 1 h is the optimal choice for the synthesis of PC.

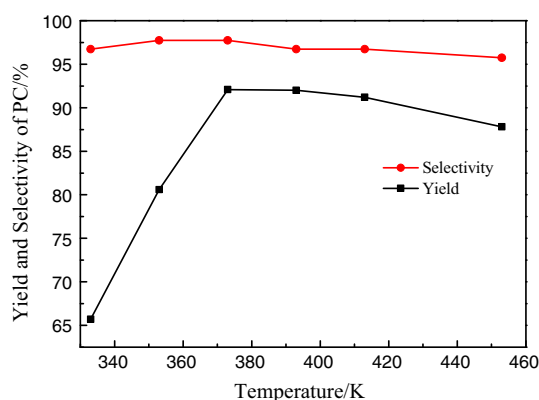


Fig. 5 Effect of temperature. Reaction conditions: catalyst **1e** (0.04 mol%), PO (0.5 mol), PC (3 mol), CO_2 pressure (4.0 MPa), reaction time (1 h)

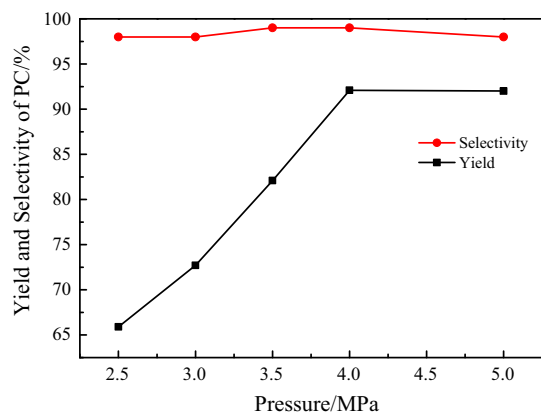


Fig. 6 Effect of CO₂ pressure. Reaction conditions: catalyst **1e** (0.04 mol%), PO (0.5 mol), PC (3 mol), temperature (373 K), reaction time (1 h)

3.4 Catalyst Recycling

A catalyst with reasonably long lifetime is critical for practical applications. Thereafter, a series of runs with catalyst **1e** were used to investigate the reusability of the catalyst under the optimized conditions. After the first reaction, the liquid was collected and distilled under reduced pressure. The products were removed and the remaining mixture including the complex catalysts were used for performing the next run. All of the reactions maintain the same proportion among the catalyst, PO and PC. The results are shown in Fig. S1. After four times of reuse, it was found that, the catalytic activity was slightly decreased, and the selectivity to PC reaches about 97 % in each run.

3.5 Catalytic Activity of Various Epoxides with CO₂

In order to test the adaptability to different epoxides, other epoxides including styrene oxide and ethylene oxide were

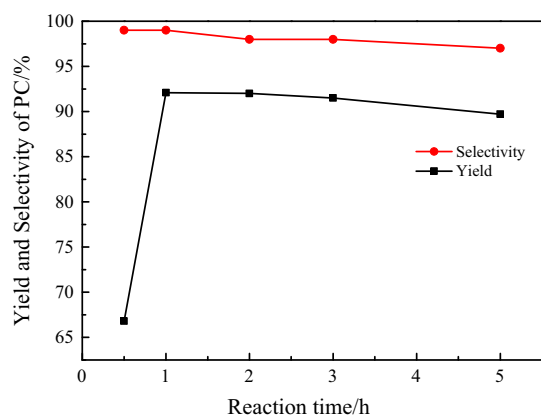


Fig. 7 Effect of reaction time. Reaction conditions: catalyst **1e** (0.04 mol%), PO (0.5 mol), PC (3 mol), temperature (373 K), CO₂ pressure (4.0 MPa)

examined under the optimized reaction conditions in the presence of **1e**, and the results are summarized in Table S3. The results indicate that the activity of ethylene oxide is high, and 90.2 % yield of ethylene carbonate was achieved in 1 h. A more higher temperature would be more suitable for the synthesis of styrene carbonate.

3.6 Corrosion Inhibition

The steel materials are usually used as the reactor materials, because of a relatively higher pressure, economic accounting standpoint in large scale chemical application. Therefore, in our system, the corrosion of the catalytic component Zn²⁺ and Br⁻ ions to the structure materials of the reactor has also been considered before its application in large scale. Here, the corrosion rates of **3**, **1e**, and the comparative KI/PEG400 catalysts in the liquid phase of PC system under the reaction conditions have been determined by the weight-loss method, and the results are presented in Table 3.

The results show the average corrosion inhibition efficiencies, thus, calculated as a function of inhibitor. For the catalyst KI/PEG400, the corrosion speed values of 1.62×10^{-2} g/(m² h) is found for the carbon steel, while the corrosion speed of the third generation catalyst **3** is more severer than the second generation catalyst. For similar concentration levels, the inhibition efficiency obtained with catalyst **1e** considerably lowermost values reported for other. The corrosion speed decreases 7.46×10^{-3} g/(m² h) for carbon steel, while it is reduced twice than KI/PEG400 and almost five times than **3**. In addition, an identical trend is observed for stainless steel. These results indicate that the N-donor ligand 1MI is an efficient inhibitor.

4 Discussion

In view of literature, catalytic activity and corrosion are hard to compromise. Therefore, our strategy is to promote the catalytic activity under mild reaction conditions and minimize the corrosion of the catalyst to the reactor materials simultaneously. Focusing on the possibility of increasing the electrophilicity of the metal complexes by introducing electron withdrawing groups, we developed a series of new dual-ligand zinc complexes, containing synergistic effects of phosphine and N-donor ligands, while the N-donor ligand also acts as inhibitor.

To pick out the most effective promotional ligand, effects of various N-donor ligands in catalytic performance have been investigated. Under the reaction conditions shown in Table 1, a synergistic effect of MTPB and N-donor ligands (1MI) was found by compared entry **1e**

Table 3 Corrosion inhibition of the catalysts in PC system

Reaction systems	KI/PEG400		3		1e	
	10 ^a	316 ^a	10	316	10	316
Coupons number	1571	5018	1572	5019	1573	5020
Before reaction (g)	20.8928	22.2830	20.8612	22.3258	20.9346	22.3553
After reaction (g)	20.8900	22.2828	20.8536	22.3249	20.9331	22.3552
Corrosion speed (g/(m ² h))	1.62 × 10 ⁻²	9.93 × 10 ⁻⁴	3.76 × 10 ⁻²	4.47 × 10 ⁻³	7.46 × 10 ⁻³	4.97 × 10 ⁻⁴

Reaction conditions: PC (4 mol), catalyst (0.04 mol%), n(KI):n(PEG400) = 1:3, temperature (418 K), time (72 h), stirring speed 20 r min⁻¹ with the acidic environment of constantly introducing CO₂ gas

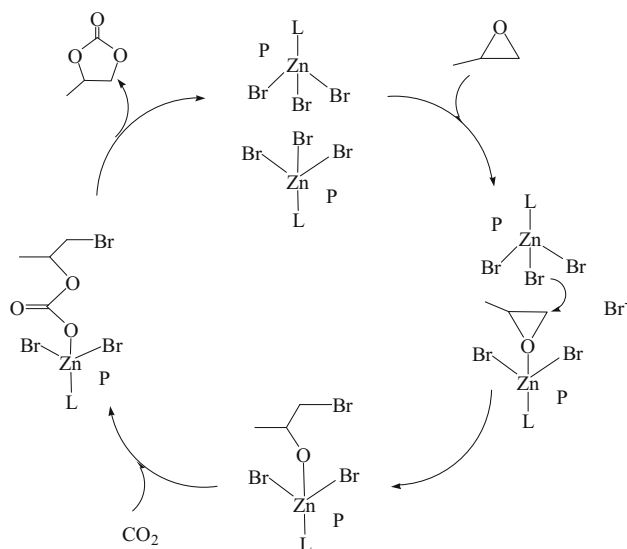
^a 10 (carbon steel): Standard NO. GB/T699-1999; 316 (stainless steel): Standard No. GB/T 20878

and **4**. The crystal structure have shown that IMI coordinates with zinc to form a mono-chelate ring complex, while the independent (MTP)⁺ cation charges balance with the anions. When there is only IMI, it would coordinate with zinc to form a bis-chelate ring complex. As a result, leaving from the metal center is not easy for the ligand. Therefore, it is difficult to offer a coordination vacancy for the formation of the reaction intermediates. It is surprising that the catalytic activity of **1d** is very low. It has been reported that IM molecules could form a long chain structure in solution by means of intermolecular hydrogen-bond formation, which might prevent the coordination of reactants [34]. This may also be true for **1f** catalyst, but the methyl steric hindrance may be have some suppressive effect on the hydrogen bonding interaction as a result of a considerable activity. The position of methyl group on imidazole has great effect on the catalytic activities. The basicity of DMI is stronger than IMI. Compared with **1e** when the attack of PO on the zinc center complex for **1g**, the steric hindrance of the ortho-position methyl will block one of the entry path onto the zinc center. The steric effect of different position methyl may explain the different enhanced catalytic activities of imidazoles except the effect of hydrogen-bond. The yields of PC decrease when N-donor ligands were used, especially the DMAP ligand, which has a strong basicity (pK_a = 9.70). In a previous report on the coupling reaction with ZnBr₂Py₂ [43, 44], it was proposed that the dissociation of a pyridine ligand followed by the coordination of PO to the zinc center and the subsequent nucleophilic attack of the carbon atom of the coordinated epoxide by the dissociated pyridine. However, the dissociation of the N-donor ligand would be more difficult for the complex bearing strongly basic N-donor ligands, because these ligands tend to form stronger bonds with a Lewis acidic zinc center. This may also explain why the **1h** complex exhibited a lower activity than the other strong basicity complexes. In polydentate ligands, the promoting effect of Phen is higher than others. This may be due to the suitable basicity, chelating

power and steric hindrance of Phen. As described above, these give the reasons why various N-donor ligands exist different enhanced catalytic activity from the side of macroscopic ligand with various pK_a values.

To study the mechanism of the enhanced catalytic activity, crystal structure was confirmed by X-ray diffraction (Fig. 3). Generally speaking, the activity of the complex results from the possibility of a dissociation of a bromine ligand from the zinc centre thereby forming a cationic zinc species, which can coordinate PO, and a free bromine anion, which is then able to ring-open the PO. This theory is supported by the crystal structure of **1e**, which exhibits an extremely long and therefore labile Zn–Br bond, and the interaction forces may be greatly weakened when there have ligands because of the diversification of bond angles and the interplay between the steric hindrance. Hence, the catalytic performance can be improved. According to the mechanism of the (salen) Cr-catalysed asymmetric ring-opening reaction in which the complexed chromium serves as a Lewis acid for PO binding/activation and simultaneously as the delivery agent for the nucleophile, which opens the PO [45–47]. On the basis of this information we propose a mechanistic model similar to those models proposed previously by Darensbourg and Yarbrough. The weak Zn–Br bond of **1e** allows an attack of the PO on the zinc center and a complex catalyst molecule opens the ring. After CO₂ insertion, back-biting process occurs which reforms the catalyst thus producing PC (Scheme 3). This mechanism suggests that a dual-ligand zinc complex system could be substituted for the reaction, in which it exists as homogeneous complex catalyst.

It should be stated that with the addition of the N-donor ligand to prepare the dual-ligand single crystal catalyst, the corrosion was significantly inhibited (Table 3). Somasundaran and co-workers [48, 49] reported that the severe corroding effect of halogen ions can be significantly restricted by adsorbing organic molecules on the metal surfaces. Our present work suggests that carbon steel and stainless steel themselves alone are inadequate for being used as the reactor



Scheme 3 Mechanistic proposal for the coupling of epoxides and CO₂

material when **3** is used as the catalyst. Nevertheless, when 1MI is added to the catalytic system, the corrosion of **1e** catalyst to carbon steel and stainless steel become very light, and hence they can be used as the reactor materials. The reduction in the corrosion may be due to the adsorption of 1MI on the metal surface, preventing the pitting corrosion of the material. Zhu et al. [50] reported the use of PEG as an effective co-catalyst, giving a 100 % conversion of PO using 1 mol% of PEG (Mn 400) and 0.33 mol% of KI at 2 MPa CO₂ pressure and 423 K after 5 h. A reduction in temperature to 373 K caused the conversion to drop to 75 % after 5 h. In comparison with the catalyst KI [50–53], under lower temperature, **1e** exhibits an equal level on catalytic activity, but a lower corrosion speed. This work also provides a concept for the development of introducing different roles of ligands in designing metal complex catalysts for the synthesis of cyclic carbonates.

5 Conclusions

In summary, several dual-ligand zinc complex catalysts, which contain phosphine and various p*K*_a N-donor ligands have been prepared and characterized them successfully, and the X-ray crystallography studies of the complex provide us a way to understand the reaction mechanism from the molecular structure aspect. A remarkable enhancement of the catalytic performance when they act as catalysts for the chemical fixation of CO₂ to PC under relatively mild conditions and the corrosion of the reaction system was effectively inhibited when 1MI was used as a N-donor ligand.

6 Supplementary Material

CCDC 1048010 contains the supplementary crystallographic data for this paper. These data can be obtained free of charge from The Cambridge Crystallographic Data Centre via www.ccdc.cam.ac.uk/data_request/cif.

Acknowledgments We acknowledge financial support of this work by the Distinguished Youth Foundation of Jiangsu Province (BK20130045), the Fok Ying-Tong Education Foundation (141069), the National High Technology Research and Development Program of China (863 Program, 2013AA032003), the National Basic Research Program of China (973 Program, 2013CB733504), the Project of Priority Academic Program Development of Jiangsu Higher Education Institutions (PAPD) and Six talent peaks project in Jiangsu Province (No. 2014-XCL-016).

References

- Sakakura T, Choi JC, Yasuda H (2007) *Chem Rev* 107:2365
- North M, Pasquale R, Young C (2010) *Green Chem* 12:1514
- Omae I (2012) *Coord Chem Rev* 256:1384
- Dai WL, Luo SL, Yin SF, Au CT (2009) *Appl Catal A Gen* 366:2
- Sakakura T, Kohno K (2009) *Chem Commun* 11:1312
- Clements JH (2003) *Ind Eng Chem Res* 42:663
- Darensbourg DJ, Holtcamp MW (1996) *Coord Chem Rev* 153:155
- Ratzenhofer M, Kisch H (1980) *Angew Chem Int Ed* 19:317
- Ratzenhofer M, Kisch H (1980) *Angew Chem* 92:303
- Gibson DH (1996) *Chem Rev* 96:2063
- Ulusoy M, Sahin O, Kilic A, Buyukgungor O (2011) *Catal Lett* 141:717
- Ema T, Miyazaki Y, Taniguchi T, Takada J (2013) *Green Chem* 15:2485
- Decortes A, Castilla AM, Kleij AW (2010) *Angew Chem Int Ed* 49:9822
- Ghosh A, Ramidi P, Pulla S, Sullivan S, Collom S, Gartia Y, Munshi P, Biris A, Noll B, Berry B (2010) *Catal Lett* 137:1
- Sun J, Han L, Cheng W, Wang J, Zhang X, Zhang S (2011) *ChemSusChem* 4:502
- He LN, Yasuda H, Sakakura T (2003) *Green Chem* 5:92
- Paddock RL, Nguyen ST (2001) *J Am Chem Soc* 123:11498
- Lu XB, Liang B, Zhang YJ, Tian YZ, Wang YM, Bai CX, Wang H, Zhang R (2004) *J Am Chem Soc* 126:3732
- Aida T, Inoue S (1983) *J Am Chem Soc* 105:1304
- Kim HS, Kim JJ, Lee BG, Jung OS, Jang HG, Kang SO (2000) *Angew Chem* 39:4096
- Zhang YY, Chen L, Yin SF, Luo SL, Au CT (2012) *Catal Lett* 142:1376
- Paddock RL, Nguyen ST (2004) *Chem Commun* 14:1622
- Calo V, Nacci A, Monopoli A, Fanizzi A (2002) *Org Lett* 4:2561
- Kawanami H, Sasaki A, Matsui K, Ikushima Y (2003) *Chem Commun* 7:896
- Decortes A, Martinez Belmonte M, Benet-Buchholz J, Kleij AW (2010) *Chem Commun* 46:4580
- Barkakaty B, Morino K, Sudo A, Endo T (2010) *Green Chem* 12:42
- Dharman MM, Yu JI, Ahn JY, Park DW (2009) *Green Chem* 11:1754
- Sun J, Fujita SI, Zhao F, Arai M (2005) *Appl Catal A Gen* 287:221

29. Li F, Xia C, Xu L, Sun W, Chen G (2003) *Chem Commun* 16:2042
30. Kim HS, Kim JJ, Kim H, Jang HG (2003) *J Catal* 220:44
31. Li F, Xiao L, Xia C, Hu B (2004) *Tetrahedron Lett* 45:8307
32. Darensbourg DJ, Yarbrough JC (2002) *J Am Chem Soc* 124:6335
33. Allen SD, Moore DR, Lobkovsky EB, Coates GW (2002) *J Am Chem Soc* 124:14284
34. Mo WL, Xiong H, Li T, Guo XC, Li GX (2006) *J Mol Catal A Chem* 247:227
35. Kim HS, Bae JY, Lee JS, Kwon OS, Jelliarko P, Lee SD, Lee SH (2005) *J Catal* 232:80
36. Sun J, Wang L, Zhang S, Li Z, Zhang X, Dai W, Mori R (2006) *J Mol Catal A Chem* 256:295
37. Katritzky AR (1963) *Physical methods in heterocyclic chemistry*. Academic Press, NY
38. Linstrom PJ, Mallard WG (2001) *J Chem Eng Data* 46:1059
39. Wang RM, Li SB, Wang YP, Chang Y, He YF, Lei ZQ, Feng HX (1999) *React Funct Polym* 42:87
40. Mostafa MF, Youssef AA, El-Dean TS, Mostafa AM, Farag IS (2007) *Z Naturforsch Sect A J Phys Sci* 62:549
41. Sun J, Han L, Cheng W, Wang J, Zhang X, Zhang S (2011) *ChemSusChem* 4:502
42. Tsang CW, Baharloo B, Riendl D, Yam M, Gates DP (2004) *Angew Chem Int Ed* 43:5682
43. Kim HS, Kim JJ, Kwon HN, Chung MJ, Lee BG, Jang HG (2002) *J Catal* 205:226
44. Kim HS, Kim JJ, Lee SD, Lah MS, Moon D, Jang HG (2003) *Chem A Eur J* 9:678
45. Hansen KB, Leighton JL, Jacobsen EN (1996) *J Am Chem Soc* 118:10924
46. Jacobsen EN (2000) *Acc Chem Res* 33:421
47. Martinez LE, Leighton JL, Carsten DH, Jacobsen EN (1995) *J Am Chem Soc* 117:5897
48. Schmid GM, Huang HJ (1980) *Corros Sci* 20:1041
49. Wei ZQ, Duby P, Somasundaran P (2003) *J Colloid Interf Sci* 259:97
50. Zhu H, Chen LB, Jiang YY (1996) *Polym Adv Technol* 7:701
51. Shi J, Song J, Ma J, Zhang Z, Fan H, Han B (2013) *Pure Appl Chem* 85:1633
52. Rokicki G, Kuran W, Pogorzelska-Marciniak B (1984) *Monatsh Chem* 115:205
53. Ma J, Song JL, Liu HZ, Liu JL, Zhang ZF, Jiang T, Fan HL, Han BX (2012) *Green Chem* 14:1743